N87-26421

SUPERSTRUCTURE HIGH EFFICIENCY PHOTOVOLTAICS*

M.Wagner, L.C. So, and J.P. Leburton
University of Illinois
Urbana, Illinois

A novel class of photovoltaic cascade structures is introduced which features multijunction upper subcells. These Superstructure High Efficiency Photovoltaics (SHEP's) exhibit enhanced upper subcell spectral response because of the additional junctions which serve to reduce bulk recombination losses by decreasing the mean collection distance for photogenerated minority carriers. Two possible electrical configurations were studied and compared: a three-terminal scheme that allows both subcells to be operated at their individual maximum power points and a two-terminal configuration with an intercell ohmic contact for series interconnection. The three-terminal devices were found to be superior both in terms of Beginning-of-Life efficiency and radiation tolerance. Realistic simulations of three-terminal AlGaAs/GaAs SHEP's show that one sun AMO efficiencies in excess of 26% are possible.

INTRODUCTION

Although considerable effort has been devoted to the development of monolithic III-V cascade cells with two energy gaps, experimentally attainable conversion efficiencies have, to date, been substantially lower than the best single-gap cells. The highest reported efficiency for a two-terminal AlGaAs/GaAs cascade cell under one-sun AMO conditions is 15.1% [ref. 1]. Lattice-mismatched AlGaAs/InGaAs cells have achieved efficiencies of only 13.6% (under one sun AM1.5 conditions) [ref. 2].

There are two principal obstacles which must be surmounted before practical monolithic cascade cells can become realizable: upper subcell quality must be improved and a low-resistance intercell ohmic contact (IOC) technology must be developed [ref. 1]. In this paper we present a novel class of cascade cells designed to overcome both problems. These superstructure high efficiency photovoltaics (SHEP's) feature an upper subcell with multiple junctions for improved performance. Previous work by the authors has shown that multiple junctions in a single-gap cell can substantially improve spectral response, particularly for AlGaAs cells of the composition needed for the upper subcell of a cascade device.

A two-terminal configuration is possible for the SHEP's, but they lend themselves most naturally to a three-terminal configuration. This might seem a serious drawback since three-terminal photovoltaics have been dismissed as impractical by many authors [refs. 1,2,4]; however, this apparent difficulty lead us to an approach which circumvents the need for an IOC with its attendant electrical and optical losses. Complementary pairs (npn and pnp) of three-terminal cells in which the upper-subcell short-circuit current of one is matched to the lower-subcell short-circuit current of the other can be used to obtain a two-terminal output. Figure 1 shows the electrical configuration and one possible physical configuration of this scheme. We found only one reference to this idea in the literature [ref. 5], so it appears to have been largely overlooked.

* Work supported by the National Aeronautics and Space Administration

DEVICE STRUCTURE AND MODELLING

Cross-sectional views of two possible SHEP structures are shown in figure 2. The five- and seven-layer structures allow both the upper-subcell emitter and lower-subcell base to be p-doped, which is desirable for optimum spectral response (electron diffusion lengths are usually longer than hole diffusion lengths in III-V compounds). Additional junctions in the upper subcell of the seven-layer structure prevent transport of collected carriers in the direction transverse to the layers, as occurs in conventional solar cells. Instead, carriers must be transported in the layer planes to heavily doped contact regions extending vertically through the superstructure. These regions are known as selective electrodes since they connect to layers of like doping, while forming reverse-biased junctions (during normal operation) with layers of opposite doping type. By allowing collected carriers to be transported in the layer planes, selective electrodes make it possible to incorporate any number of epitaxial layers in the upper subcell. Fabrication of selective electrodes in structures with doping concentrations similar to what one would expect for photovoltaics ($> 10^{18} cm^{-3}$) was recently reported [ref. 6].

The performance potential of the cells was evaluated by means of a detailed computer model, which allows a wide variety of multilayer, multi-bandgap structures to be investigated. Effects of the selective electrode regions on the minority-carrier distribution are assumed to be negligible, permitting a one-dimensional analysis. Doping and composition profiles are assumed to be uniform within each layer and abrupt at junctions. These assumptions allow closed-form expressions to be used for the contributions of each layer to short-circuit current, injection current, and space-charge recombination, so that layer thicknesses can be rapidly optimized. The optimization criterion used was to maximize beginning-of-life (BOL) efficiency with the subcells operating at their respective maximum-power points. This criterion does not yield a precise estimate of cell performance in a complementary configuration, which will require the pnp and npn cells to be simultaneously optimized because of the current-matching requirement already discussed. However, it will provide a basis for comparing the five- and seven-layer structures as well as a rough prediction of the efficiency in the complementary configuration (within 1% AMO).

The current-voltage (I-V) characteristics of the three-terminal SHEP's are represented by an Ebers-Moll model. The coupled-diode equations are:

$$J_1(v_1,v_2)=J_{sc_1}-J_{o_{11}}e^{\lambda v_1}-J_{o_{12}}e^{\lambda v_2}-\sum_m J_{gr_m}\left|\frac{e^{\frac{\lambda v_1}{2}}}{v_{b_m}-v_1}\right| \tag{1}$$

$$J_2(v_1,v_2)=J_{sc_2}-J_{o_{21}}e^{\lambda v_2}-J_{o_{22}}e^{\lambda v_1}-\sum_m J_{gr_m}\left|\frac{e^{\frac{\lambda v_2}{2}}}{v_{b_m}-v_2}\right| \tag{2}$$

where λ = q/kT and the subscript one refers to the upper subcell. The terms J_{SC_1} and J_{SC_2} represent the upper and lower subcell short-circuit current densities, respectively. Coefficients $J_{o_{11}}$, $J_{o_{12}}$, $J_{o_{21}}$ and $J_{o_{22}}$ determine the dependence of the injected component of the dark current on the subcell terminal voltages. Coupling of the I-V equations arises from interaction of the injected minority-carrier populations across the heterojunction separating the upper and lower subcells. The space-charge recombination component of the dark current is represented by the remaining terms. Each summation is over the homojunctions contained in the corresponding subcell. Note that it is necessary to have a term for each junction because, in general, the barrier potentials (V_{b_m}'s) will not be the same for all junctions in a particular subcell. If they were identical, the voltage dependent terms would factor out and one could simply sum over the J_{gr_m}'s to obtain a composite coefficient as in the case of the short-circuit and injected current terms. To compute the J_{gr_m}'s we use Choo's theory of space-charge recombination for abrupt, asymmetrical junctions [ref 7].

Expressions for the contributions of the window, emitter (upper subcell), and base (lower subcell) to the short-circuit and injected currents are well known and have been published elsewhere [8]. Contributions of layers bounded above and below by homojunctions are easily derived from the minority-carrier continuity and current-density equations with the boundary condition of zero excess carrier density at the depletion-region edges. The contributions of layers adjacent to the isotype heterojunction which separates the upper and lower subcells are considerably more complicated to calculate because one must account for interaction between the minority-carrier populations in the layers above and below the heterojunction. The barrier seen by minority carriers at the heterojunction is the junction built-in potential. This holds under all bias conditions since doping concentrations in the layers forming the heterojunction are sufficiently high that junction bias will be effectively zero for typical current densities. The boundary conditions on the minority- carrier populations are therefore

$$\frac{P_{n_2}}{P_{n_1}} = \exp[q\,(E_{F_1} - (\Delta E_v + E_{F_2}))/kT] \tag{1}$$

$$D_{P_1} \nabla P_{n_1} = D_{P_2} \nabla P_{n_2} \tag{2}$$

The fermi levels E_{F_1} and E_{F_2} are measured from the respective valence band edges. Subscript one denotes the higher gap layer of the upper subcell. These boundary conditions are nearly identical to those described for low-high junctions [ref. 9]. The only difference is the ΔE_v term which must be included in the expression for the junction barrier potential to account for the valence band edge discontinuity at the heterojunction. We assume that ΔE_v is 40% of the energy gap difference in accordance with recent experimental work [ref. 10].

For all designs studied, the top layer is specified to be a 300 Å $Al_{0.9}GA_{0.1}As$ window with a surface recombination velocity of $10^6 cm/s$. The antireflection coating is Si_3N_4 and grid obscuration is assumed to be 4%, attainable with existing grid array technology [ref. 11]. The absorption coefficient is modelled as in reference 12.

RESULTS AND DISCUSSION

We found that efficiencies of optimized SHEP structures vary gradually with upper subcell composition (figure 3). Broad peaks occur at AlAs mole fraction x = 0.36 for both the five- and seven-layer structures with maximum BOL one-sun AMO efficiencies predicted to be slightly in excess of 26%. Dependence of efficiency on composition is expected to become more critical when the current-matching constraints of the complementary design are imposed. The spectral response of a five-layer SHEP with optimum upper subcell composition (x = 0.36) is shown in figure 4. Curves for the individual layer contributions include both depletion and quasi-neutral region response.

The performance, as diffusion lengths are degraded, of two SHEP structures and a five-layer, series-connected AlGaAs-GaAs cascade cell is shown in figure 5. With space-charge recombination suppressed (fig. 5a) the seven-layer SHEP has considerably higher BOL efficiency than the five-layer structure. This is because the injection component of the dark current depends strongly on layer thicknesses, so that the effect of thinner layers in the upper subcell more than offsets the effect of having two additional junctions in that subcell. Unfortunately, the space-charge recombination component of the dark current, which tends to dominate the injection component at the maximum- power point in AlGaAs cells, is quite independent of layer thicknesses. The seven-layer SHEP is, therefore, at a slight disadvantage in BOL efficiency because of the two additional junctions if the effects of space-charge recombination are included (fig. 5b), but its overall performance is still seen to be superior to that of the five-layer SHEP.

Although simulation of a complementary pair has not yet been performed, the efficiency is expected to be very close to that of an AlGaAs-GaAs cascade cell with an ideal IOC. The curves in figure 5 were calculated using this assumption of an electrically and optically lossless IOC. The BOL efficiency of this

cell is slightly less than 27% without space-charge recombination, which is somewhat lower than the value of 27.6% found in an earlier study of AlGaAs-GaAs cascade cells (this study neglected effects of space-charge recombination) [13]. The optimum upper-subcell composition predicted by our model (x = 0.38) was also found to be somewhat lower than that of the previous study (x = 0.41). These differences are probably accounted for by the assumption in our model that diffusion lengths fall exponentially with increasing AlAs mole fraction, which tends to skew the optimum upper-subcell composition to smaller values.

It is interesting to compare the degradation curves of the two five-layer structures. The slopes are seen to be almost identical. This shows that the number of layers is more important than electrical configuration (two-terminal vs. three-terminal) in determining radiation tolerance. It should be noted that the IOC of the series-connected cell is assumed to remain ideal even as layer diffusion lengths are degraded. We therefore anticipate that complementary pairs of multilayer SHEP's will decisively outperform cascade cells with monolithic IOC's, because of the additional layers and the lack of an IOC which could undergo degradation.

CONCLUSIONS

We have presented a class of structures designed to surmount the principal difficulties facing the development of practical lattice-matched monolithic cascade cells. Upper subcell quality is improved by multiple junctions, and the problem of an IOC is completely circumvented by using complementary pairs of three-terminal cells. Although simulation of complementary cells has not yet been performed, results from series-connected structures with an ideal IOC indicate that BOL efficiencies in excess of 25% under one-sun AMO conditions should be attainable. With higher concentration factors we anticipate conversion efficiencies approaching 30%. The seven-layer SHEP appears most advantageous, at present, for space applications because of its superior tolerance to radiation degradation. If the effects of space-charge recombination were reduced, which would entail reduction of deep level impurities and vacancies, structures with even greater numbers of thinner layers could substantially increase performance.

References

1. Hutchby, J. A.; Markunas, R. J.; Timmons, M. L.; Chiang, P. K.; and Bedair, S. M.: A Review of Multijunction Concentrator Solar Cells. Proc. 18th IEEE Photovoltaic Spec. Conf. (IEEE, New York, 1985), p. 20.
2. Lewis, C. R.; Ford, C.W.; Virshup, G. F.; Arau, B. A.; Green, R. T.; and Werthen, J. G.: A Two-Junction Monolithic Cascade Solar Cell in a Lattice-Matched System. Proc. 18th IEEE Photovoltaic Spec.Conf. (IEEE, New York, 1985), p. 20.
3. Wagner, M. and Leburton, J. P.: Superstructures and Multijunction Cells for High Efficiency Energy Conversion. Proc. 18th IEEE Photovoltaic Spec. Conf. (IEEE, New York, 1985), p. 157.
4. Fan, J. C. C.; Tsaur, B-Y. and Palm, B. J.: Optimal Design of High-Efficiency Tandem Cells. Proc. 16th IEEE Photovoltaic Spec. Conf. (IEEE, New York, 1982), p. 692.
5. Sakai, S. and Umeno, M.: Theoretical Analysis of New Wavelength-Division Solar Cells. J. Appl. Phys., 51, p. 5018 (1980).
6. Dohler, G. H.; Hasnain, G.; and Miller, J. N. In Situ Grown-In Selective Contacts to NIPI Doping Superlattice Crystals Using Molecular Beam Epitaxial Growth Through a Shadow Mask. Appl. Phys. Lett., 49, p. 704 (1986).

7. Choo, S. C.: Carrier Generation-Recombination in the Space-Charge Region of an Asymmetrical p-n Junction. Solid-State Electron., 11, p. 1069 (1968).

8. Hovel, H. J.: Semiconductors and Semimetals. (Academic Press, New York, 1975) Vol. 11.

9. Godlewski, M. P.; Baraona, C. R.; and Brandhorst, H. W.: Low-High Junction Theory Applied to Solar Cells. Proc. 10th IEEE Photovoltaic Spec. Conf., p. 40 (1973).

10. Wang, W. I.: On the Band Offsets of AlGaAs/GaAs and Beyond. Solid-State Electron. Vol. 29, p. 133 (1986).

11. Werthen, J. G.; Virshup, G. F. ; Ford, C. W.; Lewis, C. R.; and Hamaker, A. C.: 21% (One-Sun air mass zero) 4 cm^2 GaAs Space Solar Cell. Appl. Phys. Lett. 48, 74 (1986).

12. Hutchby, J. A.; and Fudurich, R. L.: Theoretical Analysis of $Al_x Ga_{1-x}$ As-GaAs Graded Bandgap Solar Cell. J. Appl. Phys. 47, p. 3140 (1976).

13. Lamorte, M. F.; and Abbott, D. H.: Window Losses and Current Mismatch Computer Modeling Studies in AlGaAs-GaAs Cascade Solar Cell. IEEE Trans. Electron Devices. ED-30, p. 1313 (1983).

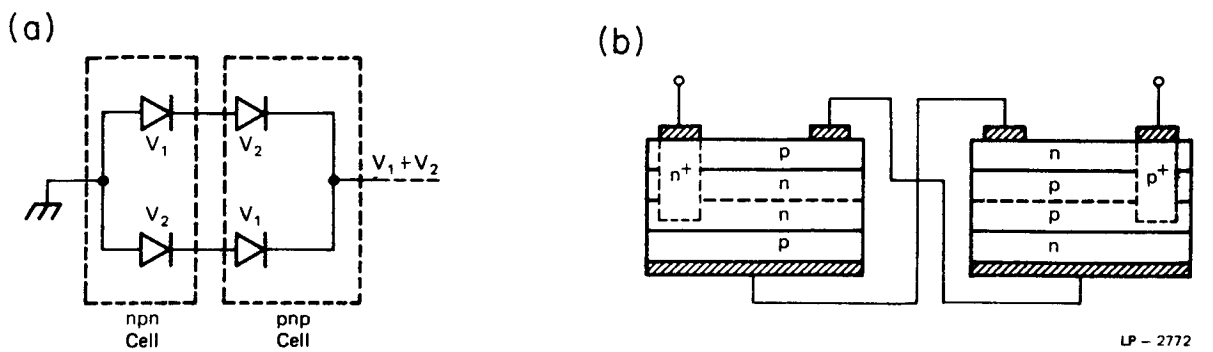

Figure 1. Complementary interconnection scheme for three-terminal photovoltaics showing a) electrical configuration and b) one possible physical configuration.

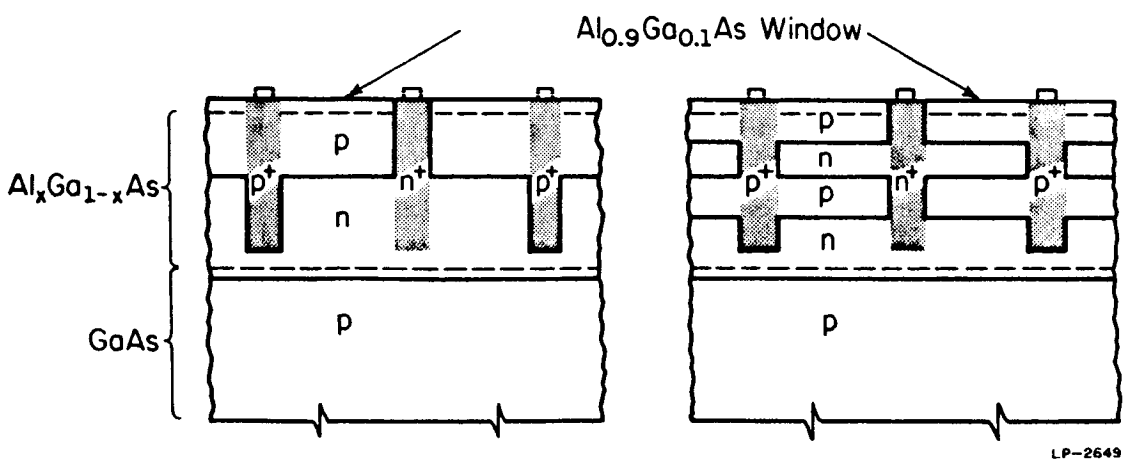

Figure 2. Cross-sectional views of five- and seven-layer SHEP structures. Isotype heterojunctions are represented by dashed lines.

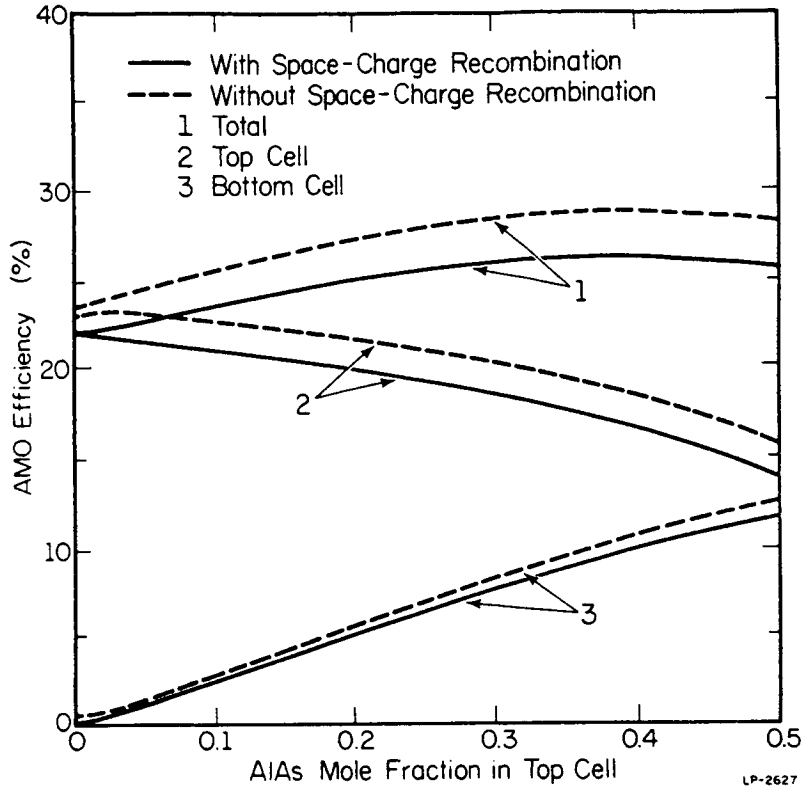

Figure 3. Performance of seven-layer SHEP structures under one-sun AMO illumination at 300 K.

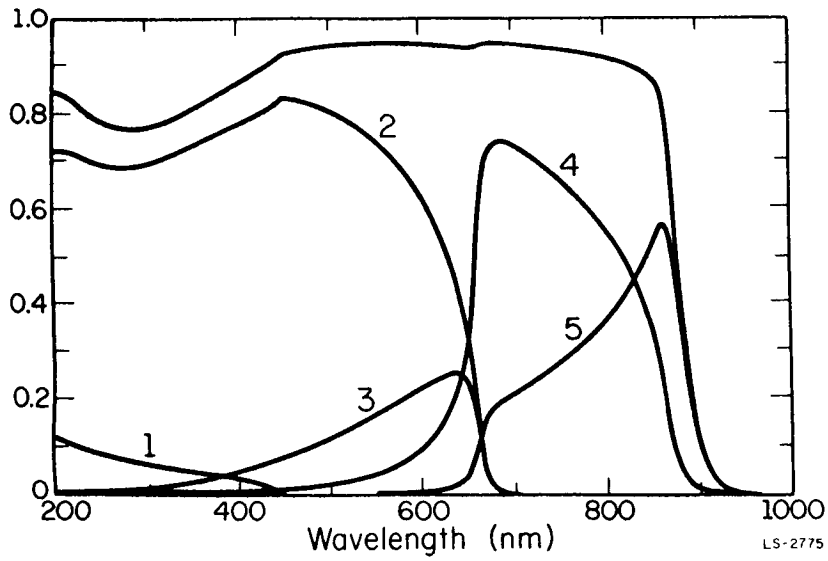

Figure 4. Spectral response of a five-layer SHEP with upper subcell composition x = 0.36. Individual layer contributions are shown as well as overall spectral response. Layers one, two, and three are the window, emitter, and base, respectively, of the upper subcell; layers four and five are the emitter and base of the lower subcell.

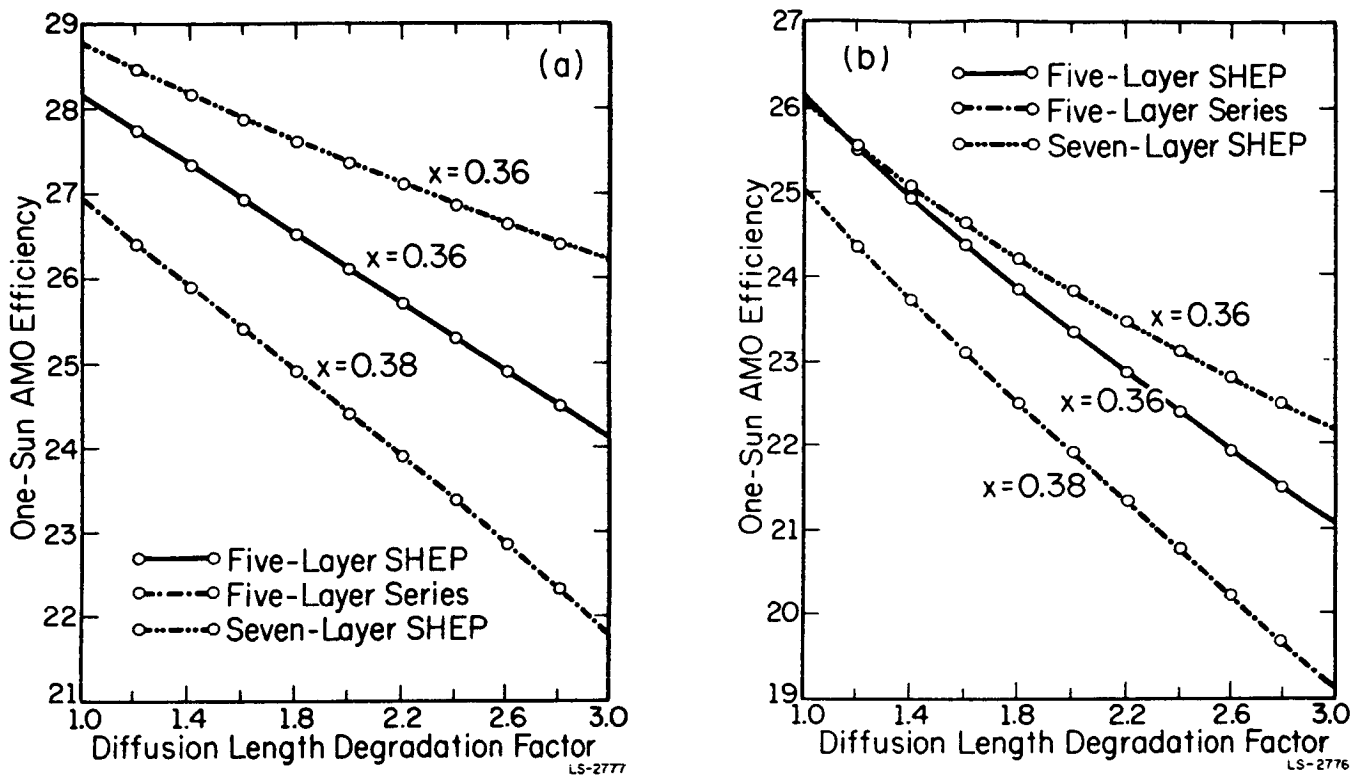

Figure 5. Performance as diffusion lengths are degraded of five- and seven-layer SHEP designs and a five-layer series-connected cascade cell with ideal IOC a) with space-charge recombination suppressed and b) including space-charge recombination.